Construction and Building Materials 207 (2019) 630–639

Contents lists available at ScienceDirect

Construction and Building Materials

journal homepage: www.elsevier.com/locate/conbuildmat

Effect of steel fiber and carbon black on the self-sensing ability of concrete cracks under bending

Yining Ding [a,*], Genjin Liu [a], Abasal Hussain [a], F. Pacheco-Torgal [b], Yulin Zhang [c]

[a] State Key Laboratory of Coastal and Offshore Engineering, Dalian University of Technology, Dalian 116024, China
[b] University of Minho, C-TAC Research Centre, Guimaraes, Portugal
[c] University of Minho, Centre of Mathematics, Braga 4700-052, Portugal

HIGHLIGHTS

- Crack self-sensing ability of concrete beam added with SF, CB and CF is studied.
- Two models for FCI-COD curve are found for deflection softening/hardening beam.
- Signal noise of FCI-COD curves has been analyzed by the fractal geometry method.
- Hybrid use of CB and SF is an optimization option for crack self sensing concrete.

ARTICLE INFO

Article history:
Received 15 July 2018
Received in revised form 24 February 2019
Accepted 25 February 2019

Keywords:
Steel fiber
Carbon black
Crack sensing of concrete
COD – FCI relation, noise signal
Fractal dimension

ABSTRACT

This work explores the mechanical and self monitoring performance of concrete beams containing steel fiber (SF), carbon black (CB) and carbon fiber (CF), when subjected to bending. The effect of the utilization of multiphase conductive materials on the compressive strength of the concrete and the load - deflection - fractional change in impedance (FCI) relationship of the concrete beam are investigated. The relationships between FCI and crack opening displacement (COD) and sensitivity (gauge factor) are also studied. Moreover, the quantitative analysis of signal noise in FCI-COD curves has been accomplished by the fractal geometry method. The result shows that a monotonic linearity and bi-linearity increasing relationship between FCI and COD can be observed for beams with deflection-softening (Group A and Group B specimens) and deflection-hardening (Group C specimens) behavior, respectively. The diphasic conductive admixture (SF + CB) improves the FCI-COD curve with higher sensitivity and lower noise signal compared to the monophasic conductive admixture (SF) and the triphasic conductive admixture (SF + CB + CF) specimen.

1. Introduction

The monitoring of crack development is of great importance for the compliance of the serviceability limit state and for the maintenance of durability requirements in concrete member. Embedded or attached sensors have been used for measuring the load, displacement, strain and other signals in structural health monitoring (SHM) projects. One of the new approaches proposed two decades ago is the use of cementitious-based materials as self-monitoring sensors [1].

Researchers have investigated the piezoresistivity of cementitious materials and its applications in SHM [2,3]. Significant advances in this field are credited to Chung and other scholars [4–8], particularly in cement and mortar containing carbon fibers. Prior works have documented the strain sensing ability of short carbon fiber (CF) cementitious materials; Chung reported that cement-based materials exhibit piezoresistivity with sufficient magnitude and reversibility [5,9]. Azhari and Banthia's study found that a cementitious based sensor carrying a hybrid of both carbon fiber and carbon nanotubes responds well to an applied compressive strain by depicting a reduction in its resistivity [10]. These studies on utilizing piezoresistivity of the conductivity phase of reinforced mortar have focused on both properties: compression and tension strain sensing and damage detection performance. However, it has been found that the strain monitoring ability range is mainly limited to the elastic stage before cracking, and the short carbon fibers are incapable to bridge the macro crack if they are pulled out from the cementitious matrix, likely cutting off the conducting path [11].

* Corresponding author.
E-mail address: ynding@hotmail.com (Y. Ding).

https://doi.org/10.1016/j.conbuildmat.2019.02.160
0950-0618/

Moreover, short CF is a brittle material, which does not strongly improve the toughness of cementitious matrix. One way to enhance the crack-bridge ability and toughness of cementitious materials is to add macro steel fibers (SF) into the matrix. There are some investigations regarding the method of enhancing the ductility of cementitious materials [12–14]. Nguyen and Song [15,16] found a good performance in the damage-sensing ability of strain-hardening SF reinforced fine aggregate concrete specimens under direct tension, and noticed that there exists a strong correlation between the electrical resistivity and the tensile elongation of the specimen. Hou [17] investigated the sensitivity of tensile strain sensors fabricated by the engineered cementitious composites and found that the gauge factor in the strain hardening region is about 3–4 times higher than that in the pre-cracking region.

Some investigations focused on the conductive pathways of cementitious materials [18–20]. Based on the literature [18], three conduction pathways have been identified: 1) a continuous conductive path (CCP) connected by a series of continuous electrolyte-filled pores; 2) a discontinuous conductive path (DCP) by blocked electrolyte-filled pores; and 3) an "insulator" conductive path (ICP) with the continuous concrete matrix. The conductivity of concrete is dominated by ionic conduction [19,20] through CCP. For concrete containing conductive materials, the conductive paths are improved. The electronic conduction tends to be strengthened by the conductive materials. Fig. 1(a) shows the conductive network of triphasic materials (Carbon black (CB) + CF + SF) in the concrete matrix before cracking [21].

In the whole process after the cracking of the concrete beam, only the macro SF is capable to restrict the crack widening, to improve the cracking resistance and toughness, to demonstrate a stable load–deflection curve and to maintain the conductive path of the cracked concrete matrix (Fig. 1(b) and (c)) while the CB and micro CF is incapable to cross the crack surfaces [21].

Actually, it is important to realize that the flexural member of conventional concrete usually works with cracks in the service stage. In fact, the self-monitoring ability of conventional concrete with coarse aggregate is less focused. Also, little attention has been paid to the electrical behavior of deflection-hardening concrete with multiple cracks, including in pre-crack and post-crack periods. Ding [21] studied the self-sensing ability in the single-crack development of concrete member with conductive materials as well as coarse aggregate under flexure, the relationship between FCR and COD was suggested and the problem of the noise signal for FCI-COD curves was mentioned qualitatively.

Based on the previous investigations, two main objectives, such as the influence of hybrid conductive materials (SF, CB and CF) on the self monitoring ability to the crack development (including the single-crack and multiple-cracks) and the noise signal of FCI-COD curve of concrete beams subjected to bending have been studied quantitatively in this work. The effect of multiphase conductive materials on the relationships of Load - Deflection - FCI, FCI – COD and sensitivity has been investigated. The noises of the FCI-COD relationship are analyzed using the fractal geometry method and demonstrate that the synergistic use of nano carbon black and steel fiber reveals a positive hybrid effect on the reduction of the noise signal.

2. Experimental investigations

2.1. Materials and mixture design

The base mix design of concrete without conductive materials is listed in Table 1. The concrete is made with P.O42.5R Portland cement. The fine aggregates are quartz sand and have a fineness modulus of 2.51 with particle size in the 0–5 mm range. The coarse aggregates used are of crushed limestone with a particle size between 5 and 10 mm. The conductive admixtures CF, CB and SF are added to enhance the conductivity and the mechanical behavior of the concrete.

Carbon black (Fig. 2 (a)), with a maximum particle size of 90 nm and a density of 0.5 g/cm^3 is used. The CB volume resistivity is of 2.3 Ω·cm. The carbon fibers (Fig. 2(b)) used in this experiment possess a diameter of 12 μm and a length of 6 mm. The density of CF is of 1.6 g/cm^3 with a volume resistivity of 10^{-3} Ω·cm. Steel fibers (Fig. 2(c)) with a diameter of 0.55 mm and length of 35 mm are used. The density of SF is of about 7.85 g/cm^3 and the volume resistivity is of approximately 10^{-5} Ω·cm. Methylcellulose is used in the amount of 0.4% by mass of cement. When CF is added, defoamer is used in the amount of 0.19% of sample volume. The different dosages of the conductive admixtures SF, CF, and CB in various concrete samples are compared and listed in Table 2. The volume resistivity of dried concrete without conductive materials usually ranges between 6 and 11 × 10^5 Ω·cm, and the volume resistivity of dried concrete with electric conductive materials usually ranges between 1 and 8 × 10^3 Ω·cm.

2.2. Samples and set-up description

A forced mixer is used for mixing. The 100 mm × 100 mm × 100 mm cube specimens for compression strength are tested at the age of 28 days. Specimens designed for bending testing are beams with the size of 100 mm × 100 mm × 400 mm. The beams are demolded 24 h after

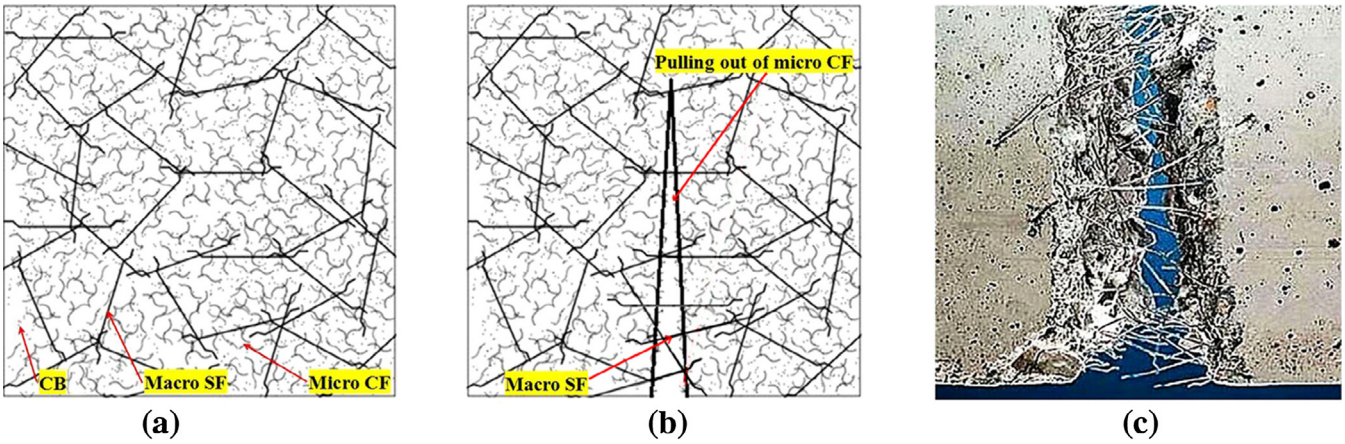

Fig. 1. Conductive network of triphasic materials in the concrete matrix (a) before cracking, (b) after cracking, (c) macro SF cross concrete crack [21].

Table 1
Base mix design of concrete.

Cement kg/m^3	Fly ash kg/m^3	Water kg/m^3	Fine aggregate (0–5 mm) kg/m^3	Coarse aggregate (5–10 mm) kg/m^3	SP kg/m^3	Water/Binder
390	155	272.5	848	822	5.5	0.5

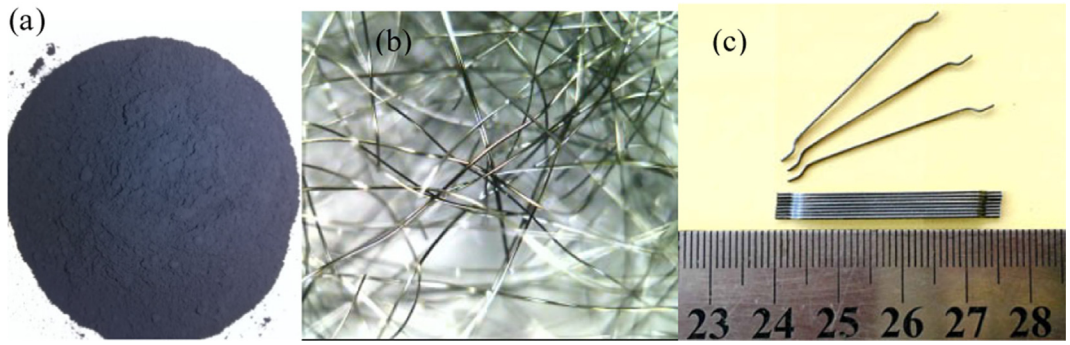

Fig. 2. Conductive materials (a) Carbon black; (b) Carbon fiber; (c) Steel fiber.

Table 2
Comparison of the content of the conductive admixtures unit (kg/m^3).

Type	Specimen	Steel fiber (SF)	Carbon black(CB)	Carbon fiber(CF)
Monophasic conductive admixture	SF20	20	–	–
	SF40	40	–	–
	SF60	60	–	–
Diphasic conductive admixture	SF20B1	20	1	–
	SF40B1	40	1	–
	SF60B1	60	1	–
Triphasic conductive admixture	SF20B1CF2	20	1	2
	SF40B1CF2	40	1	2
	SF60B1CF2	60	1	2

Definition: SF, CF and CB stands for steel fiber, carbon fiber and carbon black, the number followed with the letters stands for the content of conductive materials, kg/m^3; For example, SF60B1CF2 means the specimen with 60 kg/m^3 steel fibers, 1 kg/m^3 carbon black and 2 kg/m^3 carbon fibers.

casting and then cured at room temperature (25) (relative humidity of 100%) for 28 days. The impedance is measured by using the four-electrode-AC method, four conductive adhesive types are prepared as electrical contacts and are designated A, B, C and D. A and D (190 mm apart) are designed for passing alternating current (50HZ), while contacts B and C (100 mm apart) serve the purpose of measuring voltage. Voltmeter equipment V_1 is designed for monitoring the voltage between the inner contacts B and C. V_2 is used for measuring the voltage of the fixed resistor (R_f). The current is calculated by measuring the voltage drop across the fixed resistor allowing the electrical impedance between the inner contacts of the specimen to be calculated through Ohm's law.

The relationship between FCI (Fractional change in impedance) and load - deflection has been investigated. The relationship between FCI and COD (crack opening displacement) has also been analyzed. Details of the testing set-up are shown in Fig. 3(a).

2.3. Bending test

The specimens of concrete with different conductive admixtures are tested under flexure over a span of 300 mm in four-point bending using an hydraulic servo testing machine [22]. The close-loop test is controlled by displacement, and the deformation rate of mid-span is 0.2 mm/min. Two LVDTs are applied on the two opposite sides for measuring the mid-span deflection. An extensometer is attached at mid-span to measure the crack opening displacement during the test and the test set-up is shown in Fig. 3(b). The IMC Intelligence Data Collecting System is used to collect the data in real time.

3. Experimental results and discussion

3.1. Influence of conductive admixture on mechanical behavior

The precondition for adding functional materials into concrete to improve its conductivity is that these functional materials should not degrade the mechanical properties of concrete.

Short CF can decrease the shrinkage cracking, improve the durability and the freezing resistance [23]. CB may improve the toughness of the aggregate interface in the concrete matrix; it also shows some fine filler effect which can enhance the density of the concrete matrix [24]. The compression strength of concrete rises when the contents of CB, CF and BF (CB + CF) are slightly increased [11]. Nevertheless, CF and CB are brittle materials, the addition of CF and CB shows a small influence on the flexural toughness at a relatively low content.

Because of the differences in physical properties like surface friction, different amounts of CF and SF are used in fresh concrete to maintain the same workability, e.g. concrete with 50 kg/m^3 macro SF (SF50) and concrete with 3 kg/m^3 short CF (CF03). Fig. 4 demonstrates the comparisons of the relationships of load – crack opening development of a plain concrete (PC) beam, SF50 and CF03. The same base mix design was used as listed in Table 1 for these specimens. Additionally, for FRC specimens, part of the aggregates was replaced by the same volumetric percentage of fibers. Compared with PC beam, the addition of short CF shows small influence on the flexural strength and toughness [25]. Additionally, macro SF can greatly enhance the ultimate flexural load, the toughness and the post crack properties of a beam. Compared

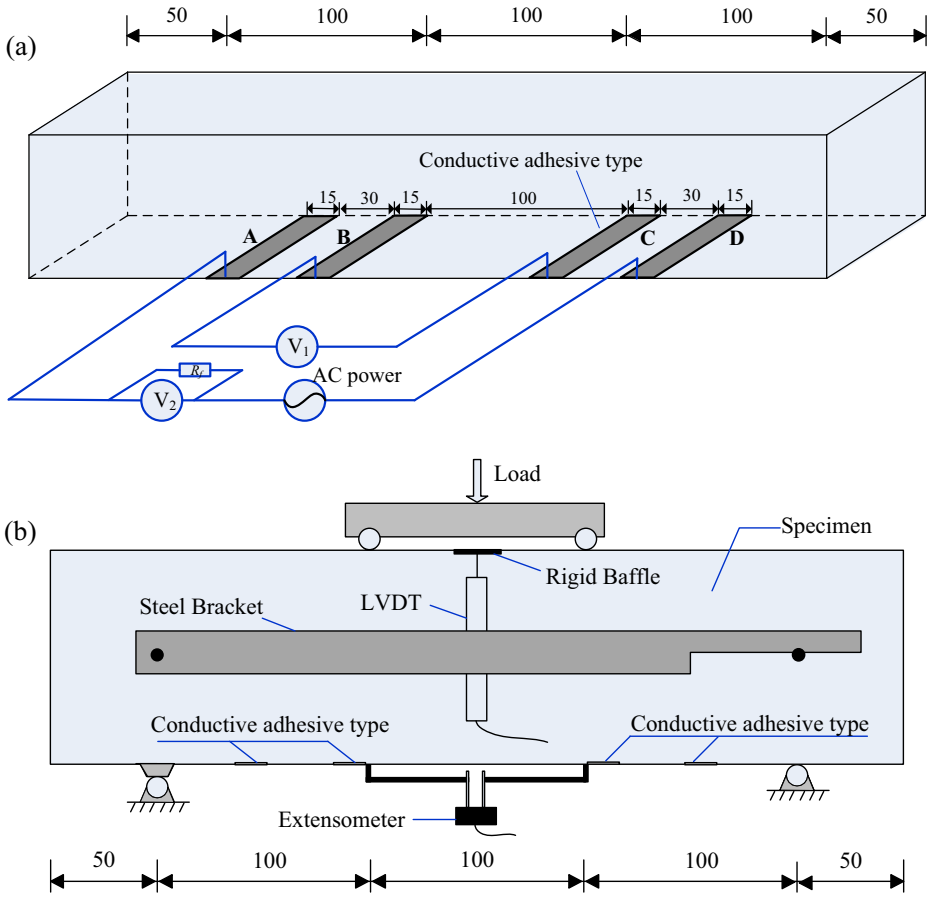

Fig. 3. Testing set-up (a) measurement of impedance; (b) measurement of load, deflection and COD.

with CF03 beam, SF50 exhibits substantially improved post-peak properties over the entire cracking region. This constitutes an important advantage of macro steel fiber. Furthermore, the previous studies declared that the addition of CB, CF and macro SF had a significant positive effect on both the flexural strength and toughness [21,26].

The compressive strength of SF reinforced concrete with and without different carbon conductive admixture is also studied. The average values of the compressive strength (f_{cu}) of three specimens are listed in Table 3. Compared to the PC specimen, the addition of conductive materials improves the compressive strength slightly.

Based on the experimental results above mentioned, the hybrid effect of carbon materials and steel fibers on the self-sensing ability to the loading capacity, deflection and crack widening as well as noise signal of concrete has been studied quantitatively in the following subsections.

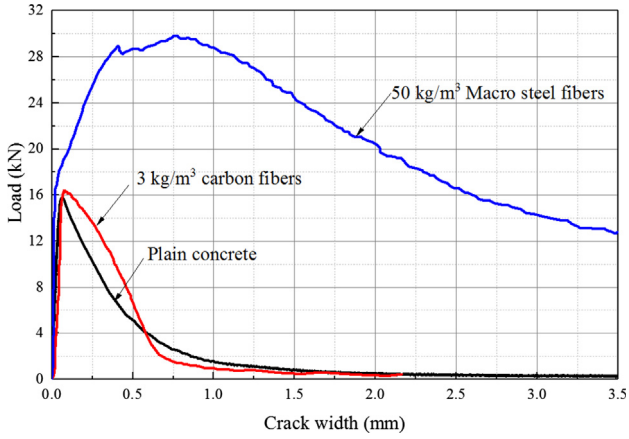

Fig. 4. Load – COD Relationship of PC, SF50 and CF03.

3.2. Effect of conductive admixtures on the relationships of FCI – deflection and load – deflection

3.2.1. Relationship of FCI – deflection and load – deflection with monophasic admixture of steel fiber only

Fig. 5(a)–(c) exhibit the effect of monophasic conductive admixtures (without carbon materials) with different SF contents (20, 40, 60 kg/m^3) on the FCI – deflection – Load curves of concrete under bending. A significant increment of FCI can be noticed during the first cracking. After cracking, an abrupt decrease of the load occurred by 52.2%, 27% and 8.9% compared with the first peak load for specimen SF 20 (Fig. 5(a)), SF40 (Fig. 5(b)) and SF60 (Fig. 5(c)),

Table 3
Comparison of the compressive strength of the concrete with different dosages of the conductive admixtures.

Series	Specimen	f_{cu} (MPa)
Reference	PC	35.4
Group A	SF20	38.3
	SF20B1	35.4
	SF20B1CF2	35.2
Group B	SF40	39.9
	SF40B1	37.9
	SF40B1CF2	37.6
Group C	SF60	37.7
	SF60B1	38.0
	SF60B1CF2	41.3

respectively. Meanwhile, the impedance of SF20, SF40 and SF60 is increased by 10.8%, 4.2% and 1.7%, respectively. It can be concluded that both the load drop rate and the impedance change during first cracking decreased with the increasing of SF content.

The bending behavior of a fiber reinforced concrete beam can be classified as deflection softening and deflection hardening. A beam undergoing deflection softening indicates less post-cracking flexural load than the cracking load. A deflection hardening beam however can possess a higher flexural load than the cracking load [27–30]. For specimen SF20 and SF40, a deflection softening behavior was observed. After the first drop, the load bearing capacity increases slightly and then decreases gradually. Correspondingly, the rise in the FCI-deflection curve from the first cracking is approximately linear. For SF60 specimen, after the first drop of load, it exhibits deflection hardening behavior with a plateau on the FCI-deflection curve (Fig. 5c). Following the peak load, the rise of FCI-deflection curve becomes steeper.

The changes in the load bearing capacity and FCI during the first concrete cracking and the value of FCI at a deflection of 2 mm (FCI_2) and 4 mm (FCI_4) are illustrated in Tab.4. For deflection control of SLS (Serviceability Limit State), the Chinese National Code GB 50010 [31] sets limit to the allowable deflection for beam with span less than 7 m as $l_0/200$ (l_0 is the span length). Based on ASTM C 1609, the load–deflection is recorded to an end-point deflection of at least 2 mm, so FCI at 2 mm deflection would be enough for sensing of $l_0/200$. But, in order to enlarge the validity of the self-sensing ability for large deformation as well as application scope of crack width, the maximum measuring deflection in our experiment is extended up to 4 mm based on RILEM recommendation [32]. So in our manuscript FCI at the 4 mm was selected to represent the sensing ability for large scope of crack width, and FCI_4 covers the region of FCI_2 and can be regarded as the boundary for the deflection sensing ability. From Table 4 it can be seen that the FCI_2 of SF20, SF40 and SF60 is 16.4%, 8.0% and 6.9%, respectively. The FCI_4 of SF20, SF40 and SF60 is 19.4%, 13.0% and 12.2%, respectively, which implies that the FCI decreases with the increasing of SF content at the same deflection. This is due to the fact that beam with high SF content provides more fibers to bridge the cracked sections, and the conductive network can be kept more stable and durable with a higher SF content than that with a lower fiber content.

3.2.2. Relationships of FCI - deflection and load – deflection with multiphase admixtures of steel fibers and carbon materials

The effect of diphasic conductive admixtures (1 kg/m^3 nano carbon black) with different SF contents on the FCI - deflection - Load curves of concrete subjected to flexure is demonstrated in Fig. 6 (a)–(c).

Fig. 6 and Table 4 show that the load drop is 8.82 kN, 5.74 kN and 1.98 kN from the first peak load of specimen SF 20B1 (Fig. 6 (a)), SF40 B1 (Fig. 6(b)) and SF60 B1 (Fig. 6(c)), respectively. Meanwhile, the impedance of SF20, SF40 and SF60 is increased by 5.7%, 2.4% and 1.8%, respectively.

Comparing the beams containing same amount of SF with and without CB, specimens with 1 kg/m^3 of nano CB exhibits higher value of FCI_2 and FCI_4 than those without CB, except for the specimen SF60B1 which has a moderate increase in FCI over the deflection range between 0.25 mm and 1.5 mm. With the addition of CB the fluctuations of the FCI-deflection curves decrease. This happens because the CB fills the microscopic space between adjacent fibers, and also, the concrete matrix. This is helpful as it provides a more stable conductive network in the concrete than the beam without CB, thus lowering the electrical noise signal.

Fig. 7(a)–(c) illustrates the influence of a triphasic conductive admixture (1 kg/m^3 nano carbon black + 2 kg/m^3 carbon fiber) with different SF contents on the FCI – deflection – Load curves of concrete when subjected to bending. The CF dosage is limited by its poor dispersion in fresh concrete.

From Fig. 7 it can be seen that the FCI - deflection curve of triphasic conductive admixture specimens shows an upward trend, similar to monophasic and diphasic conductive admixture specimen during the first cracking. Comparing specimen SF60B1CF2 with SF60B1 and SF40B1CF2 with SF40B1, the FCI_2 values increased by 94.2% and 10.3%, respectively. Furthermore, the FCI_4 of specimen SF60B1CF2 increased by 70.7% when compared to the FCI_4 of specimen SF60B1. This proves that CF is much more effective than CB and SF in providing the sensing ability. This ability comes from the pulling-out of crack-bridging carbon fibers during tension affecting the electrical contact between the fiber and cement matrix [24]. However, the FCI_2 and FCI_4 of SF20B1CF2 are decreased compared to that of SF20B1. Consequently, the CF content used in this work is not as much as in other published papers[24,33]. This may be one of the reasons for the unstable effects for CF added specimens on the deflection sensing performance.

3.3. Effect of conductive admixture on the relationship between FCI and COD

3.3.1. Two patterns of FCI - COD relationship

Fig. 8(a)–(i) illustrate the relationship between FCI and COD of the specimens. They demonstrate that the relationships between FCI and COD for group A and group B specimens (Deflection softening behavior) are different to those of the Group C specimens (Deflection hardening behavior).

For group A and group B specimens, a monotonic linear increasing relationship between FCI and COD can be observed. The gauge factor (GF) (the fractional change in impedance per unit crack opening displacement) is used to quantify the FCI - COD relationships. This can also be defined as the sensitivity and its value can

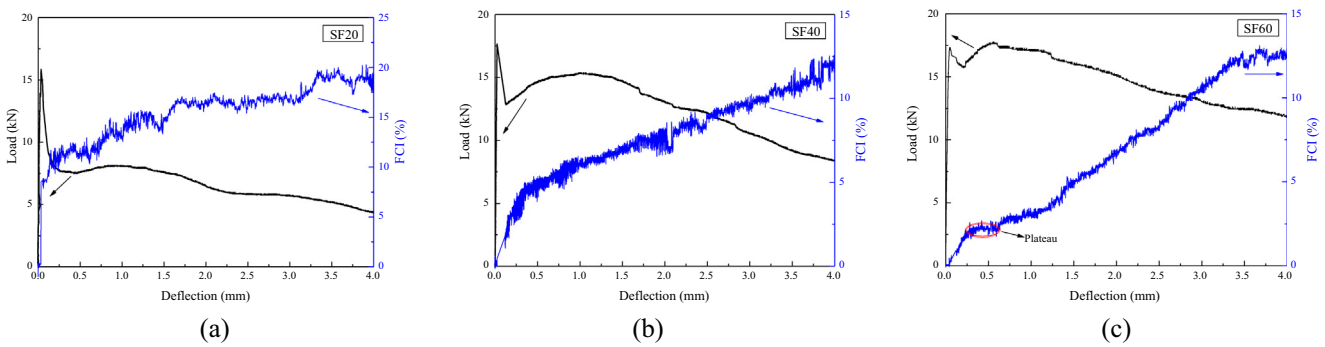

Fig. 5. Relationships between load and deflection, FCI and deflection of (a) SF20, (b) SF40, (c) SF60.

Table 4
Change of FCI and loading of the beam during the first crack and FCI_a.

Series	Specimen	Load drop (kN)	Load drop rate (%)	Increment of FCI (%)	FCI_2	FCI_4
Specimens without carbon materials	SF20	8.25	52.2	10.8	16.4%	19.4%
	SF40	4.75	27.0	4.2	8.0%	13.0%
	SF60	1.58	8.9	1.7	6.9%	12.2%
Specimens with carbon materials	SF20B1	8.82	53.1	5.7	19.8%	32.3%
	SF40B1	5.74	35.9	2.4	8.7%	17.5%
	SF60B1	1.98	10.7	1.8	5.2%	9.9%
	SF20B1CF2	8.01	49.4	3.7	5.4%	7.1%
	SF40B1CF2	7.17	37.9	4.2	9.6%	13.1%
	SF60B1CF2	0.60	3.5	1.3	10.1%	16.9%

Definition: Load drop rate is equal to (P_1-Load drop)/P_1, where P_1 is the first peak load;
FCI_a: The value of FCI at deflection of a mm.

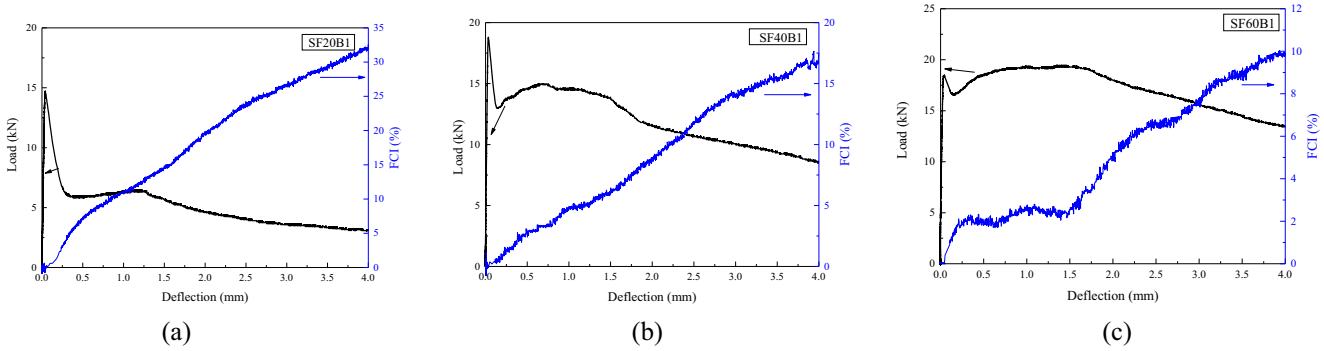

Fig. 6. Load – deflection - FCI Relationships (a) SF20B1, (b) SF40B1, (c) SF60B1.

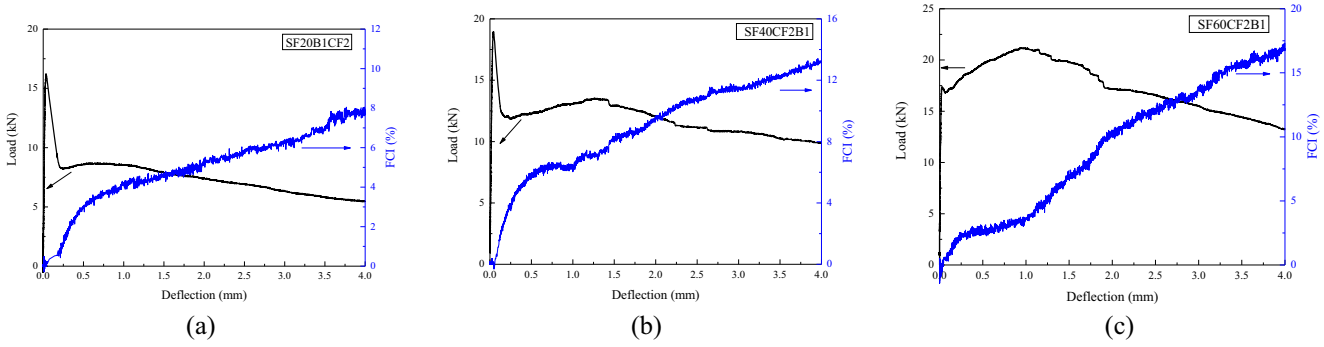

Fig. 7. Load – deflection - FCI Relationship of (a) SF20B1CF2, (b) SF40B1CF2, (c) SF60B1CF2.

be acquired from the slope of the regression line fitted to those data from FCI - COD curve for the beams with deflection softening behavior (Fig. 8(a), (b), (d), (e), (g), (h)).

For Group C specimens, bi-linear increasing relationships of FCI – COD are observed (Fig. 8(c), (f), (i)). The slope of FCI – COD curve changes when the load reaches its peak value. GF_1 is the slope of the regression line for the FCI – COD curve in the zone I, where the multiple cracks form and propagate before the peak load. GF_2 is the slope of the regression line for the FCI – COD curve in zone II, where the localization of the critical crack occurs.

The GF values are summarized in Table 5 and vary from 0.34 to 4.68. More specifically, GF_2 is larger than GF_1 for Group C specimens, i.e., GF_2 (1.89) is 5.6 times GF_1 for specimen SF60B1. This signifies that the sensitivity of the specimen in the crack localization region is higher than that in the region of the formation and propagation of the multiple cracks. This is due to the fact that in the crack localization region, the critical crack widens significantly and the conductive network is weakened (which is mainly caused by the pulling out of carbon materials and slipping of steel fibers in the matrix).

3.3.2. Effect of carbon materials and steel fibers on the gauge factor

The GF values of the specimens with and without carbon materials are compared in Table 5. It can be seen that:

- Compared with SF20, the GF of SF40 decreased by 39.3%. The existing of SF will delay the development of concrete crack. For the less fiber reinforced beam, the conductive network can be cut off rapidly, so the electrical resistance changes larger than the increased content fiber reinforced beam. This means that the rise in the SF content in concrete will reduce its cracking sensitivity. However, the GF_1 of SF60 increased by 37.9% when compared with SF40, it may because of the deflection hardening behavior.

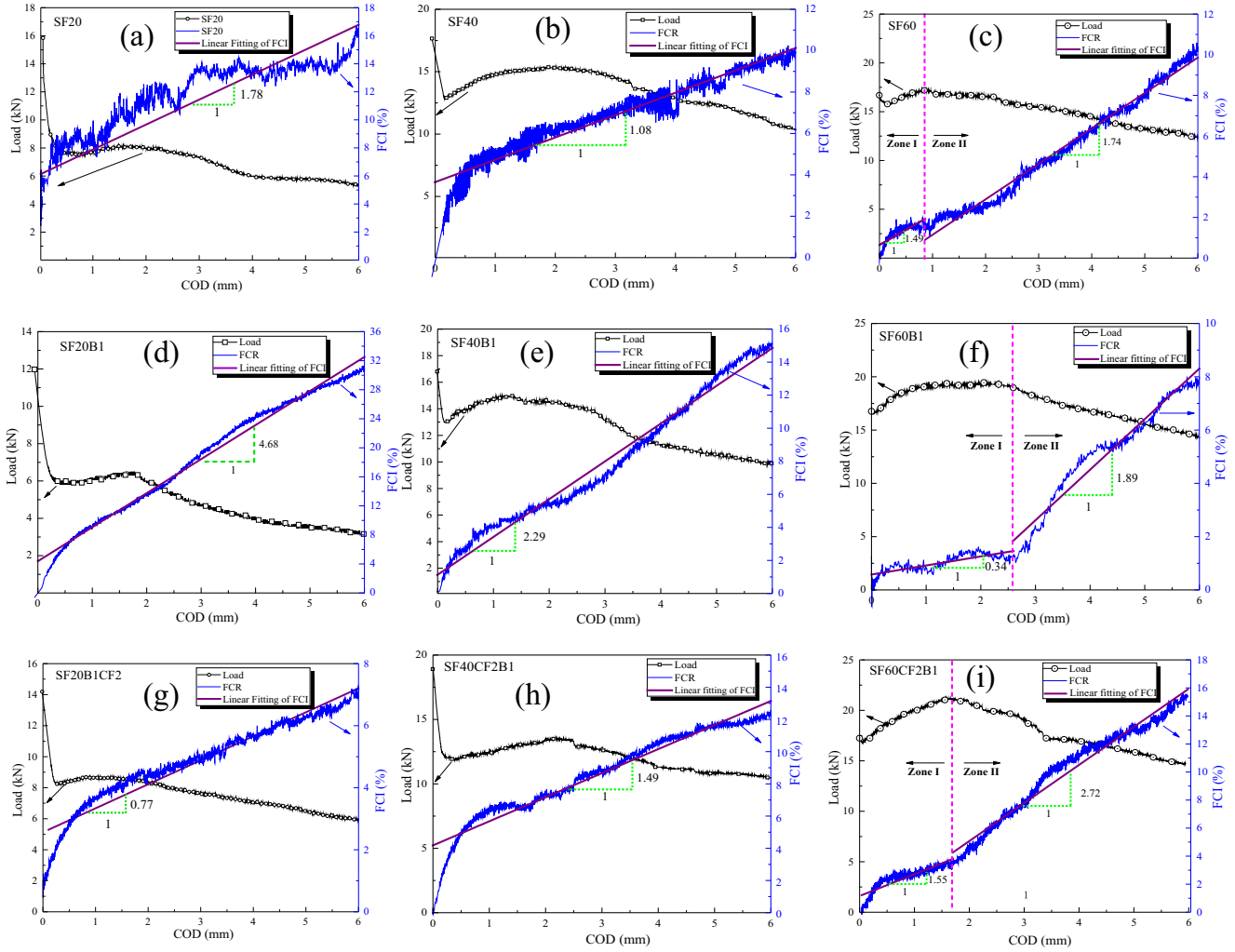

Fig. 8. Load – COD - FCI Relationships of (a) SF20, (b) SF40, (c) SF60, (d) SF20B1, (e) SF40B1, (f) SF60B1,(g) SF20B1CF2, (h) SF40B1CF2,(i) SF60B1CF2.

Table 5
Gauge factor of the specimens.

Specimen	GF	
	Zone I(GF_1)	Zone II(GF_2)
SF20	1.78	–
SF20B1	4.68	–
SF20B1CF2	0.77	–
SF40	1.08	–
SF40B1	2.29	–
SF40B1CF2	1.49	–
SF60	1.49	1.74
SF60B1	0.34	1.89
SF60B1CF2	1.55	2.72

- Comparing specimen SF20 with SF20B1 and SF40 with SF40B1, the GF values increased by 162.9% and 112%, respectively. SF20B1 possesses the highest GF when compared to the other beams. In addition, the GF_2 value of specimen SF60B1 is 8.6% higher than that of SF60. This proves that 1 kg/m^3 of CB will enhance the sensing ability of a concrete beam reinforced with steel fibers. For concrete containing CB and SF as conductive materials, a) the addition of CB improves the electrical conductivity by exhibiting short-range electron transfer ability in concrete; b) the addition of SF contributes to the formation of continuous conductive pathways by bridging up several structural cracks as well as isolated conductive clusters[33]. For the beam with 60 kg/m^3 steel fibers, the sensing ability of concrete decreased for zone I. Compared to SF20B1 (Fig. 8(d)) and SF40B1 (Fig. 8(e)), the SF60B1 (Fig. 8(f)) has a flatter multiple cracking stage while the slow widening of cracks makes the FCI increase in a moderate pattern.

3.3.3. Analysis of the noise signal of FCI-COD curves for sensing crack development

As illustrated in Fig. 8, some FCI-COD curves (Fig. 8 (a), (b), (c)) are disturbed by irregular noise signals. In order to analyze the effect of the conductive admixture on the noise signal, the tortuosity of the FCI-COD curves was investigated quantitatively by means of the fractal geometry, which is one of the useful methods to study the irregular topography [34], and the fractal dimension (D) is introduced as a geometric parameter to evaluate the noise signal.

For the characterization of FCI-COD curves, the box-dimension method (box-counting method) is applied. In order to keep the same unit scale between the coordinates of each direction in the graph, both x and y-axis of the FCI-COD curve are normalized. Fig. 9 shows the box-dimension process of the representative specimen SF40B1. The red square grids are used to cover the data of the normalized FCI-COD (represented by FCI'-COD') curves (blue

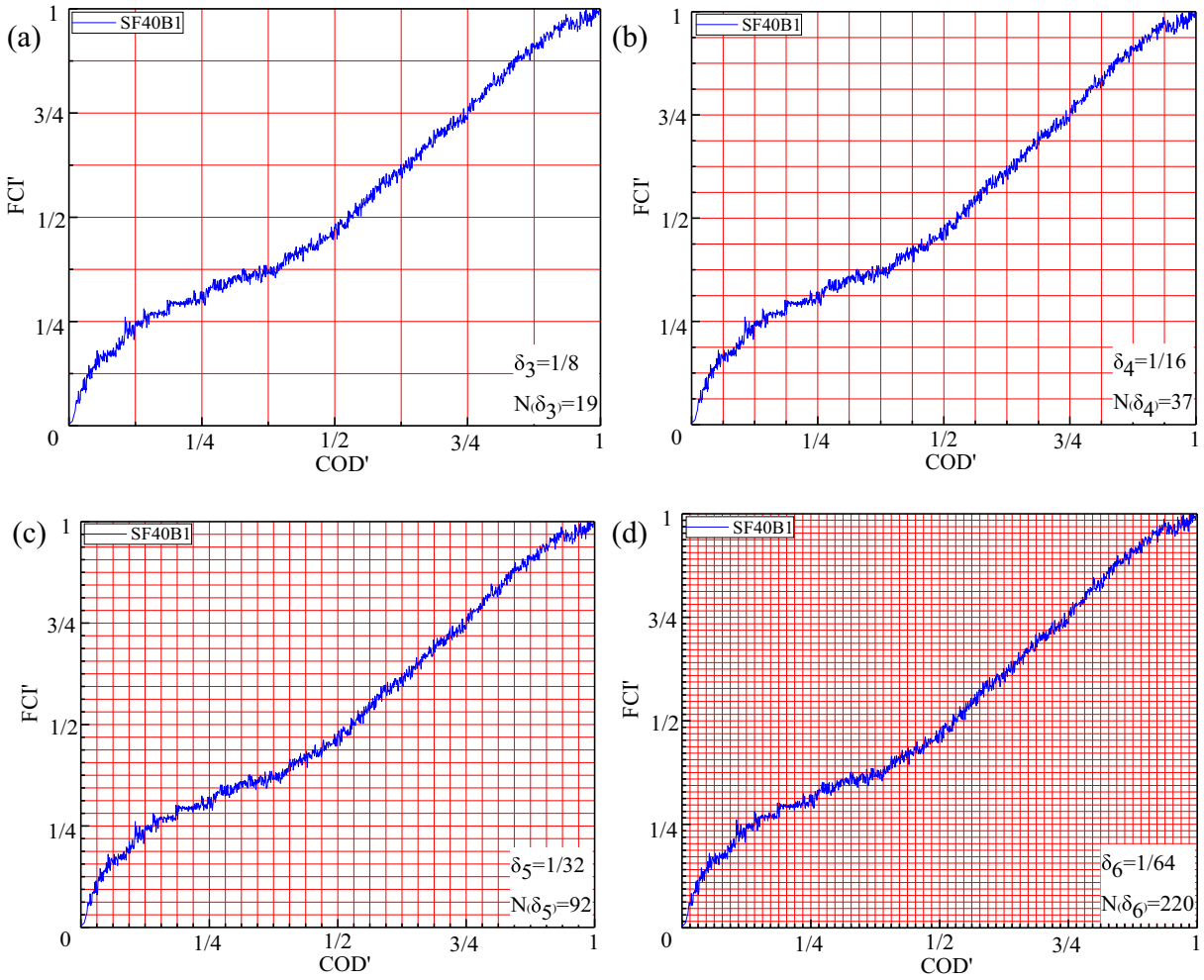

Fig. 9. Normalized FCI-COD(FCI'-COD') curve covered with different grid sizes (a) δ_3, (b) δ_4, (c) δ_5, (d) δ_6.

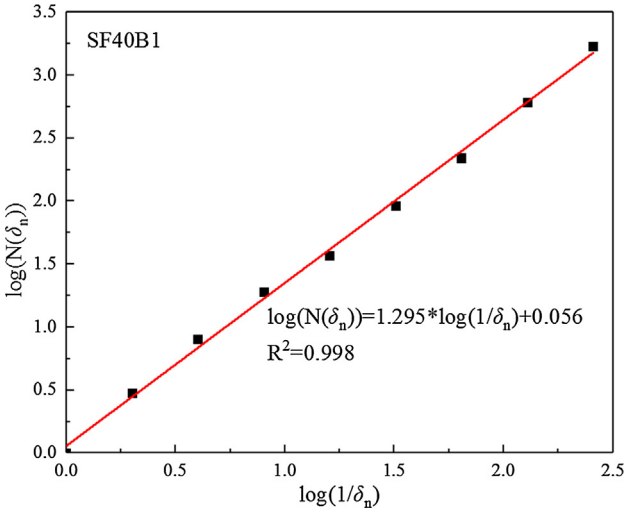

Fig. 10. Relationship between log[N(δ_n)] and log(1/δ_n).

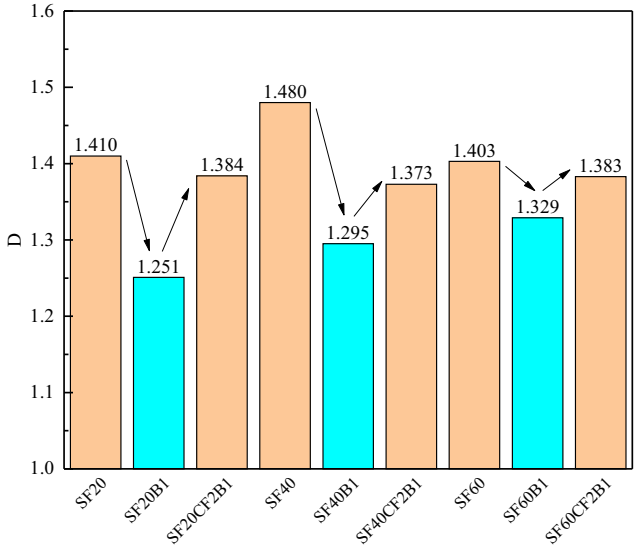

Fig. 11. Fractal dimension of the specimen.

curves) and the data containing grids are counted to accumulate. The fractal dimension (D) could be evaluated from the Eq. (1).

$$D = \lim_{\delta_n \to 0} \frac{\log N(\delta_n)}{\log(1/\delta_n)} \quad (1)$$

where, N(δ_n) is the number of grids; δ_n is the grid size and the initial grid size δ_0 is 1, $\delta_n/\delta_{n+1} = 2$; e.g. the FCI'-COD' curve of SF40B1 is covered with different grid sizes and the corresponding number of grids containing FCI'-COD' data is counted by a Matlab program.

As illustrated in Fig. 9, N(δ_3) is 19 when δ_3 is equal to 1/8, N(δ_4) is 37 when δ_4 is equal to 1/16 and N(δ_5) is 92 when δ_5 is equal to 1/32, N(δ_6) is 220 for δ_6 equals to 1/64, and so on.

The log(N(δ_n)) versus log($1/\delta_n$) plot is shown in Fig. 10, it can be seen that there is a linear correlation between log[N(δ_n)] and log ($1/\delta_n$). The slope of the log[N(δ_n)] - log($1/\delta_n$) relationship is equal to the fractal dimension D, and for SF40B1 D = 1.295. For an ideal case of a smooth straight line without any noise signal, D = 1. It means that the closer the fractal dimension D is to 1, the lower the noise signal is.

The fractal dimension of all the specimens is calculated and exhibited in Fig. 11, it can be seen that the mean values of the fractal dimension of FCI'-COD' curves for monophasic conductive admixture specimens, diphasic conductive admixture specimens and triphasic conductive admixture specimens are 1.431, 1.292 and 1.373, respectively. The diphasic conductive admixture has the lowest mean value of fractal dimension, especially for specimen SF20B1 with a value of 1.251. This implies that hybrid added CB and SF into specimen can cause lower noise signal in the FCI-COD curve when compared to monophasic (SF) and triphasic conductive admixture (SF + CB + CF). This may be attributed to the well dispersed CB particles in the matrix that fill the nano level pores to form a strong and stable conductive pathway due to their nano size [35].

The hybrid use of CB and SF into concrete can both take advantage of the conductive network of SF and also make use of the electric characteristics of CB [24]. Furthermore, the noise signal of triphasic conductive admixture is larger than the diphasic conductive admixture. As carbon fibers are difficult to disperse uniformly in concrete, and as such, some of the fibers maybe clustered together, causing the noise signal to increase.

4. Conclusions

In order to select the suitable conductive materials for crack monitoring, a series of experiments have been performed. Especially, the application of the SF, CB and CF as smart materials for self-sensing of concrete crack was explored. The experimental and analytical results have led to the following conclusions:

1. The high toughness and the multiple crack behavior of conductive concrete are mainly caused by the macro steel fibers.
2. As the load bearing capacity declines fast during the first cracking, the FCI of all beams clearly increases. For specimens with single crack, a linear increasing trend of the FCI – COD curve can be found.
3. For specimens with multiple cracks, a bi-linear increasing trend of FCI - COD relation is found, and the gauge factor/GF_2 in the post-peak region is greater than the value of GF_1 in the pre-peak region.
4. The noise signals can be well analyzed by means of the fractal dimension (D); the FCI - COD curves of beams without carbon materials demonstrate greater noise signals (D > 1.403) than those with carbon materials.
5. For concrete with diphasic conductive materials of CB and SF, the addition of 1 kg/m^3 of carbon black into the specimens may improve the self-sensing ability (GF) of concrete with different dosages of steel fibers (with an exception for the group C).
6. The diphasic use of carbon black and steel fibers into concrete may contribute to lower noise signal (D < 1.329) in the FCI-COD curve compared to monophasic and triphasic conductive admixture specimens. The diphasic use of CB and SF can be an optimization option for improving the self sensing ability of concrete in respect to crack development.

Conflict of interest

None.

Acknowledgment

The authors acknowledge the National Natural Science Foundation of China (Grant: 51578109), the National Natural Science Foundation of China (Grant: 51421064).

References

[1] P.-W. Chen, D.D. Chung, Carbon fiber reinforced concrete for smart structures capable of non-destructive flaw detection, Smart Mater. Struct. 2 (1) (1993) 22.
[2] D. Chung, Structural health monitoring by electrical resistance measurement, Smart Mater. Struct. 10 (4) (2001) 624–636.
[3] B. Han, X. Guan, J. Ou, Electrode design, measuring method and data acquisition system of carbon fiber cement paste piezoresistive sensors, Sens. Actuators, A 135 (2) (2007) 360–369.
[4] D. Chung, Strain sensors based on the electrical resistance change accompanying the reversible pull-out of conducting short fibers in a less conducting matrix, Smart Mater. Struct. 4 (1) (1995) 59–61.
[5] D.D.L. Chung, Piezoresistive cement-based materials for strain sensing, J. Intell. Mater. Syst. Struct. 13 (9) (2002) 599–609.
[6] F. Azhari 2008 Cement-based sensors for structural health monitoring. University of British Columbia, Master Degree thesis.
[7] R.M. Chacko, N. Banthia, A.A. Mufti, Carbon-fiber-reinforced cement-based sensors, Can. J. Civ. Eng. 34 (3) (2007) 284–290.
[8] B. Han, S. Ding, X. Yu, Intrinsic self-sensing concrete and structures: A review, Measurement 59 (2015) 110–128.
[9] S. Wen, D.D.L. Chung, A comparative study of steel- and carbon-fibre cement as piezoresistive strain sensors, Adv. Cem. Res. 15 (3) (2003) 119–128.
[10] F. Azhari, N. Banthia, Cement-based sensors with carbon fibers and carbon nanotubes for piezoresistive sensing, Cem. Concr. Compos. 34 (7) (2012) 866–873.
[11] Y. Ding, Z. Chen, Z. Han, Y. Zhang, F. Pacheco-Torgal, Nano-carbon black and carbon fiber as conductive materials for the diagnosing of the damage of concrete beam, Constr. Build. Mater. 43 (2013) 233–241.
[12] N. Banthia, N. Nandakumar, Crack growth resistance of hybrid fiber reinforced cement composites, Cem. Concr. Compos. 25 (1) (2003) 3–9.
[13] N. Banthia, M. Sappakittipakorn, Toughness enhancement in steel fiber reinforced concrete through fiber hybridization, Cem. Concr. Res. 37 (9) (2007) 1366–1372.
[14] N. Buratti, C. Mazzotti, M. Savoia, Post-cracking behaviour of steel and macro-synthetic fibre-reinforced concretes, Constr. Build. Mater. 25 (5) (2011) 2713–2722.
[15] D.L. Nguyen, J. Song, C. Manathamsombat, J.K. Dong, Comparative electromechanical damage-sensing behaviors of six strain-hardening steel fiber-reinforced cementitious composites under direct tension, Compos. B Eng. 69 (2015) 159–168.
[16] J. Song, D.L. Nguyen, C. Manathamsombat, D.J. Kim, Effect of fiber volume content on electromechanical behavior of strain-hardening steel-fiber-reinforced cementitious composites, J. Compos. Mater. 49 (29) (2015) 3621–3634.
[17] T.-C. Hou, J.P. Lynch, Conductivity-based strain monitoring and damage characterization of fiber reinforced cementitious structural components, Smart Struct. Mater.Sens. Smart Struct. Technol. Civil, Mech. Aerosp. Syst.: Int. Soc. Opt. Photonics 5765 (2005) 419–430.
[18] G. Song, Equivalent circuit model for AC electrochemical impedance spectroscopy of concrete, Cem. Concr. Res. 30 (11) (2000) 1723–1730.
[19] M.C. Forde, J. McCarter, H.W. Whittington, The conduction of electricity through concrete, Mag. Concr. Res. 33 (114) (1981) 48–60.
[20] D.E. Macphee, D.C. Sinclair, S.L. Cormack, An AC impedance spectroscopy study of hydrated cement pastes, Adv. Cem. Res. 10 (4) (1998) 151–159.
[21] Y. Ding, Z. Han, Y. Zhang, J. Aguiar, Concrete with triphasic conductive materials for self-monitoring of cracking development subjected to flexure, Compos. Struct. 138 (2016) 184–191.
[22] ASTM C. 1609/C 1609M Standard Test Method for Flexural Performance of Fiber-Reinforced Concrete (Using Beam With Third-Point Loading). United States, 2010.
[23] P.W. Chen, D.D.L. Chung, Low-drying-shrinkage concrete containing carbon fibers, Compos. B Eng. 27 (3–4) (1996) 269–274.
[24] S. Wen, D.D.L. Chung, Partial replacement of carbon fiber by carbon black in multifunctional cement–matrix composites, Carbon 45 (3) (2007) 505–513.
[25] Y. Ding, Z. Han, Y. Zhang, C. Azevedo, Hybrid use of steel- and carbon-fiber reinforced concrete for monitoring of crack behavior, in: ECCM15–15th European Conference on Composite Materials: European Conference on Composite Materials, 2012, pp. 1–8.
[26] Y. Ding, Y. Huang, Y. Zhang, S. Jalali, J. Aguiar, Self-monitoring of freeze–thaw damage using triphasic electric conductive concrete, Constr. Build. Mater. 101 (2015) 440–446.

[27] Pike L M. Model for predicting creep of cracked steel fibre reinforced concrete. University of Stellenbosch, Doctoral dissertation, 2018.
[28] D. Kim, A.E. Naaman, S. El-Tawil, Comparative flexural behavior of four fiber reinforced cementitious composites, Cem. Concr. Compos. 30 (10) (2008) 917–928.
[29] F.U.A. Shaikh, Deflection hardening behaviour of short fibre reinforced fly ash based geopolymer composites, Mater. Des. 50 (2013) 674–682.
[30] A.E. Naaman, Deflection-Softening and Deflection-Hardening FRC Composites: Characterization and Modeling, Special Publication 248 (2007) 53–66.
[31] Code, for design of concrete structures GB 50010–2010 2010.
[32] RILEM TC 162-TDF. Test and design methods for steel fiber reinforced concrete, bending test, final recommendation. Mater Struct 2002; 35(253):579–82.
[33] S. Wu, L. Mo, Z. Shui, Z. Chen, Investigation of the conductivity of asphalt concrete containing conductive fillers, Carbon 43 (7) (2005) 1358–1363.
[34] Y. An, K. Wu, Z. Xiong, A quantitative study on the surface crack pattern of concrete with high content of steel fiber, Cem. Concr. Res. 32 (9) (2002) 1371–1375.
[35] H. Li, H. Xiao, J. Ou, Electrical property of cement-based composites filled with carbon black under long-term wet and loading condition, Compos. Sci. Technol. 68 (9) (2008) 2114–2119.